Resistive X-point modes in tokamak boundary plasmas

J.R. Myra and D.A. D'Ippolito

Lodestar Research Corporation, Boulder Colorado

X.Q. Xu and R.H. Cohen

Lawrence Livermore National Laboratory, Livermore, CA

December 1999

(submitted to Physics of Plasmas)

DOE/ER/54392-08 LRC-99-76

LODESTAR RESEARCH CORPORATION

2400 Central Avenue

Boulder, Colorado 80301

LRC-99-76 DOE/ER/54392-08 (1999)

Resistive X-point modes in tokamak boundary plasmas

J.R. Myra, D.A. D'Ippolito
Lodestar Research Corporation, 2400 Central Ave., Boulder CO

X.Q. Xu, R.H. Cohen
Lawrence Livermore National Laboratory, Livermore, CA
(December 28, 1999)

Abstract

It is shown that the boundary (edge and scrape-off-layer) plasma in a typical L-mode diverted tokamak discharge is unstable to a new class of modes called resistive X-point (RX) modes. The RX mode is a type of resistive ballooning mode that exploits a synergism between resistivity and the magnetic geometry of the X-point region. RX modes are shown to give robust instabilities at moderate mode numbers, and therefore are expected to be the dominant contributors to turbulent diffusion in the boundary plasma of a diverted tokamak.

52.55.Fa, 52.35.-g, 52.30.Jb, 52.35.Ra

Understanding the physics of tokamak boundary [edge and scrape-off-layer (SOL)] plasmas continues to be an active and important area of fusion research. It is widely recognized that the edge plasma can control global confinement and provides a crucial and as yet poorly understood boundary condition for core transport. Turbulent transport in the SOL is thought to set the SOL width, and is therefore important when considering divertor heat exhaust issues.

The L-H transition is known experimentally to be sensitive to the presence of an X-point in the plasma, motivating the present work in which we consider the influence of the X-point geometry on plasma stability. Like earlier work,[1,2] our goal is an understanding of boundary plasma turbulence, but the present study is significantly different in that we focus here on the fundamental role of the X-point and SOL.

The collisional boundary plasma is typically well described by the reduced Braginskii fluid model.[3,4] A simplified set of model equations, adequate for the present discussion, is given by Eqs. (1) - (5) for vorticity (yielding electrostatic potential Φ), Ohm's law (parallel current density $J_\parallel$), continuity (density n), electron temperature (T_e) and vector potential $A_\parallel$:

$$\frac{c^2}{4\pi v_A^2}\left(\frac{\partial}{\partial t}+\mathbf{v}_E\cdot\nabla+\mathbf{v}_{di}\cdot\nabla\right)\nabla_\perp^2\Phi=\nabla_\parallel J_\parallel+\frac{2c}{B}\mathbf{b}\times\boldsymbol{\kappa}\cdot\nabla p, \tag{1}$$

$$\eta_\parallel J_\parallel+\frac{\partial}{\partial t}\left(\frac{J_\parallel m_e}{n_e e^2}\right)+\nabla_\parallel\Phi+\frac{1}{c}\frac{\partial A_\parallel}{\partial t}=\frac{1.71}{e}\nabla_\parallel T_e+\frac{T_e}{en_e}\nabla_\parallel n_e, \tag{2}$$

$$\left(\frac{\partial}{\partial t}+\mathbf{v}_E\cdot\nabla\right)n_e=\frac{1}{e}\nabla_\parallel J_\parallel+\frac{2c}{eB}\mathbf{b}\times\boldsymbol{\kappa}\cdot(\nabla p_e-n_e e\nabla\phi), \tag{3}$$

$$\frac{3}{2}n_e\left(\frac{\partial}{\partial t}+\mathbf{v}_E\cdot\nabla\right)T_e=\nabla_\parallel\kappa_\parallel\nabla_\parallel T_e, \tag{4}$$

$$\nabla_\perp^2 A_\parallel=-(4\pi/c)J_\parallel. \tag{5}$$

where $\mathbf{v}_E=(c/B)\mathbf{b}\times\nabla\Phi$. Neglected are the dynamics of the ion temperature and parallel velocity. A proper treatment of the ion temperature modifies the nonlinear form of the left-hand-side (lhs) of Eq. (1),[3] but the linearized equation, considered here, is unaffected. Notations are standard: v_A is the Alfven velocity, v_{di} the diamagnetic drift, $\boldsymbol{\kappa}$ is the curvature of the equilibrium magnetic field $\mathbf{B}$ and $p=nT$.

The presence of the X-point region has important consequences for wave behavior[5–11] and, by implication, for the nonlinear evolution of the boundary plasma. In lowest order, $\mathbf{k}\cdot\mathbf{B}=0=k_\zeta B_\zeta+k_\theta B_\theta$ yields $k_\theta=nB_\zeta/RB_\theta$, which is singular at the X-point where $B_\theta\to 0$. Here our orthogonal coordinate system is $(\psi,\theta,\zeta)=$ (radial, poloidal, toroidal), and n is the toroidal mode number. In eikonal theory, the $\mathbf{e}_\psi$ component of $\mathbf{k}$ may be obtained from $\mathbf{e}_\zeta\cdot\nabla\times\mathbf{k}=0$ (since $\mathbf{k}=\nabla S$ for some eikonal function S)

$$\frac{\partial}{\partial\theta}\left(\frac{k_\psi}{RB_\theta}\right) = \frac{\partial}{\partial\psi}\left(JB_\theta k_\theta\right) \tag{6}$$

where J is the Jacobian, and is found to grow dramatically along the field line near and beyond the X-point.[5,6,10]

The ramifications for stability are most easily seen from the eikonal ballooning formalism. With the neglect of $\kappa_\parallel$ in the T_e equation, a second order ordinary differential eigenmode equation results,

$$B(\omega-\omega_{dkp})\frac{v_A^2}{k_\perp^2}\nabla_\parallel\frac{k_\perp^2/B}{\omega-\omega_{Re}+\omega_\eta+\tilde{\omega}H}\nabla_\parallel\psi+[\gamma_{mhd}^2+(\tilde{\omega}+\omega_\kappa-\omega_{\kappa i})(\tilde{\omega}-\omega_{*i})]\psi=0 \tag{7}$$

where standard notations are employed (see e.g. Ref. 10) and $\tilde{\omega}=\omega-\omega_E$, $\omega_E=\mathbf{k}\cdot\mathbf{v}_E$, $\omega_\eta = i\eta_\parallel k_\perp^2c^2/4\pi$, $H=k_\perp^2c^2/\omega_{pe}^2$, $\omega_{\kappa i}=(2cT_i/eB)\mathbf{k}\cdot\mathbf{b}\times\boldsymbol{\kappa}$, $\omega_\kappa=(2c(T_i+T_e)/eB)\mathbf{k}\cdot\mathbf{b}\times\boldsymbol{\kappa}$, $\gamma_{mhd}^2 = -\omega_\kappa(\omega_{*en}+\omega_{*eT}-\omega_{*i})/[k_\perp^2\rho_s^2(1+T_i/T_e)]$, $\omega_{dkp}=\omega_{Re}+\omega_{\kappa i}-(\tilde{\omega}-\omega_{*i})k_\perp^2\rho_s^2$, $\omega_{Re}=\omega_E+\omega_{*en}+1.71\omega_{*eT}$, and the eigenfunction is $\psi=[(\omega-\omega_{dkp})/(\tilde{\omega}-\omega_{\kappa i})]$ (e ϕ_1/T_e) $\propto e\phi_1/T_e-n_1/n_0-1.71T_1/T_e$ with subscript 1 denoting perturbed quantities. The freqeuncy ω_η characterizes the effects of plasma resistivity due to electron dissipation (collisional skin effect) while H describes electron inertia (collisionless skin effect). In Eq. (7) we have made the non-essential but simplifying assumptions of neglecting parallel variations in the equilibrium n, T profiles, and some perpendicular compressibility terms associated with $\boldsymbol{\kappa}$ on the rhs of Eq. (3).

Equation (7), supplemented by appropriate boundary conditions (BCs) (evanescent ψ as $\theta\to\pm\infty$ in the edge, and[10–13] at the SOL divertor plates) has been solved by the linear shooting code BAL (a generalization of the code described in Ref. 10) which optimizes growth rates over the size and orientation of $k_\perp$ (toroidal mode number n and ballooning parameter θ_0) as well as over a range of flux surfaces encompassing about 1 cm of plasma on either side of the separatrix. Both the BAL code, and the nonlinear three-dimensional turbulence code BOUT[4,14] employ realistic magnetic geometry taken from EFIT runs for particular discharges on the DIII-D tokamak. Here we restrict attention to a typical L-mode discharge, where the effects of $E\times B$ shear on the modes are negligible and the plasma is well into the MHD stability regime.

Using experimentally measured density and temperature profiles as base case input to BAL and BOUT, we have identified five different possible instability branches in Eq. (7): ideal MHD, classical resistive MHD, drift-Alfven, SOL modes associated with sheath BCs, and resistive X-point (RX) modes. The nonlinear BOUT simulations indicate that the RX mode is the dominant instability for the DIII-D L phase discharge.

Figure 1 illustrates the basic physics of this mode on a field line approximately 1 mm inside the separatrix ($\psi=99.8\%$, the surface of maximum growth rate) where the local plasma parameters are $n_e=1.86\times10^{13}\mathrm{cm}^{-3}$, $T_e=67$ eV, $T_i=53$ eV, $L_n=2.3$ cm, $L_{te}=1.0$ cm, $L_{ti}=2.6$ cm. The most unstable mode for this case has toroidal mode number $n=30$, and growth rate $\gamma=1.2\times10^5$ s^{-1} corresponding to $\gamma/\gamma_{mhd0}=0.15$ and $\gamma/\Omega_{i0}=1.9\times10^{-3}$ where subscript 0 denotes the outboard midplane and $\Omega_i=ZeB/m_ic$. Near the outboard midplane ($\theta=\pi/2$) the mode has nearly ideal MHD behavior ($|\omega|\gg|\omega_\eta|$) and acquires its instability drive from ∇p weighted bad curvature (γ_{mhd}). The mode propagates along the field line, carrying energy up and down towards the respective X-points, as illustrated by the Poynting flux $S_\parallel=(c/16\pi)\mathbf{b}\cdot\mathbf{E}_1^*\times\mathbf{B}_1+cc.=J_{\parallel1}\phi_1^*/4+$ cc. The lower X-point at

$\theta = 0$ is in the plasma for this case; the upper one at $\theta = \pi$ is not, but its effect on the mode is still evident in Fig. 1. When the X-point region is encountered, resistive effects become important: the growth of $k_\perp^2$ causes $\omega_\eta \propto k_\perp^2$ to become large and the eigenfunction transitions from an ideal mode ($E_{\|1} = 0$) to an electrostatic one ($A_{\|1} = 0$). Beyond the X-point where $|\omega| \ll |\omega_\eta|$, resistivity allows plasma slippage through the magnetic field lines, so that ψ can become small without paying a large "line bending" penalty associated with the stabilizing second derivative term in Eq. (7).

The upper and lower X-points thus tend to confine the mode to the outboard (low-field and bad curvature) side, and further isolate the mode from the BCs which could otherwise dominate its behavior: in the edge, far from the MHD ballooning stability limit, the requirements of periodicity on an interchange-like mode are typically very stabilizing, while in the SOL the effect of sheath BCs[10–12] can often be very destabilizing. Thus the X-point dramatically affects the spatial and spectral distribution of unstable modes.[14]

The underlying physics of the RX mode and the classical resistive ballooning mode[15] is similar — both modes decay away from θ_0 (without line-bending penalty) due to resistivity, made significant by the magnetic-shear-induced growth of k_ψ. The classical resistive ballooning mode requires high n to make resistivity significant ($\omega_\eta > \omega$). In contrast, the RX mode exists for much lower n because $|\omega_\eta|$ increases by many orders of magnitude near the X-point. Thus, the effects of X-point geometry and resistivity are synergistic; resistivity is almost always important near the X-point (for any reasonable tokamak boundary plasma parameters and mode numbers). The role of an X-point on boundary plasma instabilities is treated in greater detail in a recent review article.[16] The significance, for turbulent transport, of robust instabilities at lower n is suggested by the mixing length estimate for $D \sim \gamma/k_\perp^2$.

To further explore these points, unstable spectra for typical edge ($\psi = 98\%$) and SOL ($\psi = 101\%$) flux surfaces are illustrated in Fig. 2 for both the X-point diverted geometry "X-pt" and a limiter plasma "shifted circle" geometry which has the same plasma profiles, but the magnetic geometry of shifted circle flux surfaces, with a toroidal symmetric limiter at the bottom of the machine. The X-point spectra of Fig. 2a show two RX mode branches peaking near $n = 50$, and the high-n classical branch peaking for $n > 200$. (The eigenfunction for the fastest growing low-n branch peaks at the lower X-point, while the other low-n branch peaks at the upper X-point.) In the limited plasma, (shifted circle model) the high-n branch is similar, but the low-n modes have greatly reduced growth rates relative to the X-point case. This is because the ballooning effect characterized by $\alpha = \gamma_{mhd}^2 q^2 R^2 / v_A^2$ is weak here, forcing the low-n eigenfunctions in the shifted circle case to average over favorable curvature on the inboard side of the torus. Differences between the two geometries becomes less pronounced as α increases because strong ballooning allows modes to localize to the outboard midplane in both geometries.

In contrast to the stabilizing effect of the X-point in the edge, Fig. 2b shows that the X-point reduces instability growth rates in the SOL. This occurs because the X-point isolates modes from the destabilizing boundary conditions at the divertor plate, whereas the limited plasma is subject to virulent sheath-related SOL instabilites[10–12] which capitalize on "free" ($\nabla_\| \Phi = 0$) or partially conducting boundary conditions. In Fig. 2b two unstable branches are clearly evident in the shifed circle case. The low-n branch is interchange like, with a perturbed potential that slightly favors the bad curvature side of the torus, and maximizes at the outboard side of the limiter. The higher-n branch eigenfunction is entirely localized

to the bad curvature region, is finite at the limiter and has considerably more structure.

BOUT simulations, employing a more complete set of reduced Braginskii equations than shown in Eqs. (1) - (5), (in particular, retaining full T_e, T_i and $v_{||}$ equations) have been used to investigate the nonlinear behavior of the RX mode and to allow first principles calculation of the resulting turbulent diffusion coefficient. Using experimentally measured n, T, and Φ profiles in L- and H-mode for a particular shot, which are held fixed in the code, BOUT yields ion thermal diffusivities of 0.3 m^2/s in L-mode and 0.05 m^2/s in H-mode near the separatrix,[14] which are encouragingly close to experimentally deduced values. The dynamic evolution of the L-H transition has recently been simulated in BOUT by incorporating simple sources near the core boundary and sinks in the SOL region.[4] An H-mode-like pedestal is formed with much reduced transport, and a large negative radial electric field is established near the separatrix associated with turbulence-generated plasma rotation.

In conclusion, we see that there is a fundamental synergy between resistivity and the X-point which contributes new physics to the linear instabilities and to the nonlinear evolution of the boundary plasma. We have identified the resistive X-point mode as the basic unstable mode for resistive edge and SOL plasmas in X-point geometry in the L-phase.

ACKNOWLEDGMENTS

The authors wish to thank G.D. Porter and R. Moyer for providing boundary plasma profile and magnetic geometry data for DIII-D. This work was supported by the U.S. Department of Energy (DOE) under contract/grant numbers DE-FG03-97ER54392, and W-7405-ENG-48; however this support does not constitute an endorsement by the DOE of the views expressed herein.

REFERENCES

[1] B.N. Rogers, J.F. Drake and A. Zeiler, Phys. Rev. Lett. **81**, 4396 (1998).

[2] B. Scott, in *Theory of Fusion Plasmas*, 1998, proc. of the *Joint Varenna-Lausanne International Workshop* (SIF, Bologna, 1998), p. 359.

[3] A. Zeiler, J.F. Drake, B. Rogers, Phys. Plasma **4**, 2134 (1997).

[4] X.Q. Xu, R.H. Cohen, T.D. Rognlien and J.R. Myra, invited paper, APS-DPP Conference, Seattle, WA, Nov.15-19, 1999; to be published in Phys. Plasmas

[5] D. Farina, R. Pozzoli and D.D. Ryutov, Nucl. Fusion **33**, 1315 (1993).

[6] N. Mattor and R.H. Cohen, Phys. Plasmas **2**, 4042 (1995).

[7] A.V. Nedospasov, Fiz. Plazmy **15**, 1139 (1989) [Sov. J. Plasma Phys. **15**, 659 (1989)].

[8] W. Kerner, O. Pogutse, R. van der Linden, Plasma Phys. Cont. Fusion **39**, 757 (1997).

[9] J.R. Myra and D. A. D'Ippolito, Phys. Plasmas **5**, 659 (1998).

[10] J.R. Myra, D. A. D'Ippolito and J.P. Goedbloed, Phys. Plasmas **4**, 1330 (1997).

[11] X.Q. Xu and R.H. Cohen, Contrib. Plasma Phys. **38**, 158 (1998).

[12] H.L. Berk, R.H. Cohen, D.D. Ryutov, Yu.A. Tsidulko and X.Q. Xu, Nucl. Fusion **33**, 263 (1993).

[13] R.H. Cohen and D.D. Ryutov, Plasma Phys. **2**, 2011 (1995).

[14] X.Q. Xu, R. H. Cohen, G.D. Porter, T.D. Rognlien, D.D. Ryutov, J.R. Myra. D.A. D'Ippolito and R. Moyer, presented at the *17th IAEA Fusion Energy Conf.*, Yokohama, Japan, October 1998, paper IAEA-CN-69/THP2/03.

[15] see for example T.C. Hender, B.A. Carreras, W.A. Cooper, J.A. Holmes, P.H. Diamond, and P.L. Similon, Phys. Fluids **27**, 1439 (1984); and refs. therein.

[16] J.R. Myra, D.A. D'Ippolito, X.Q. Xu and R.H. Cohen, LRC Report #LRC-99-74 DOE/ER/54392-07 (1999), to be published in Contrib. Plasma Phys.

FIGURES

FIG. 1. Variation of (a) the normalized resistive frequency ω_η/ω and (b) the resistive X-point eigenfunction ψ and normalized Poynting flux $S_\parallel/k_\perp^2$ with extended ballooning coordinate θ. Resistive effects are dominant when $|\omega_\eta/\omega| > 1$, enabling the eigenfunction to go to zero without energetically expensive line bending. The sign of $S_\parallel/k_\perp^2$ indicates the direction of energy propagation, which goes from the outboard midplane at $\theta = \pi/2$ to the lower (upper) X-point at $\theta = 0$ ($\theta = \pi$).

FIG. 2. Unstable spectra showing growth rate $\gamma(10^3/\mathrm{s})$ vs. toroidal mode number n in (a) in the edge and (b) the SOL. In each case results are shown for the full divertor geometry ("X-pt") and for limiter geometry employing a "shifted circle" flux surface model. Note that the presence of the X-point stabilizes the SOL but is destabilizing for the moderate and low-n ($n < 100$) modes in the edge. The significance of various unstable branches is discussed in the main text.

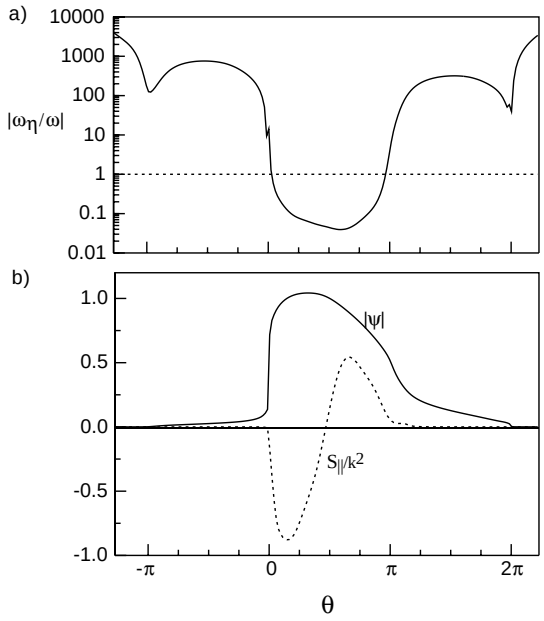

Fig. 1

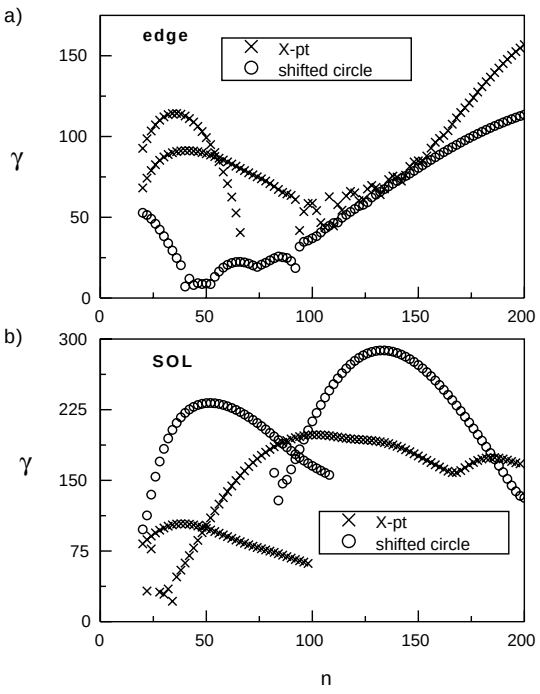
a)
edge
X-pt
shifted circle
γ
150
100
50
0
0
50
100
150
200
b)
SOL
γ
300
225
150
75
0
X-pt
shifted circle
n

Fig. 2